Journal of Newviews in Engineering and Technology (JNET)
Volume 4, Issue 3, December 2022
Available online at http://www.rsujnet.org/index.php/publications/2022-edition
e- ISSN: 2795-2215

Incipient Fault Localization and Classification for Transmission Lines using Neural Intelligent Technique.

Biobele A. Wokoma[1], Dikio C. Idoniboyeobu[2], Christopher O. Ahiakwo[3] and Sepribo L. Braide[4]
[1,2,3&4] Department of Electrical Engineering, Rivers State University
biobele.wokoma@ust.edu.ng

ABSTRACT
The problem of incipient fault localization and classification in power transmission lines is an emerging area of power system research that seeks to determine the likelihood or probability of fault just before its occurrence. This involves the determination of power line fault signatures and online characterization of line parameters. This research paper applies a simulations and data driven based approach emphasizing resonance theory of transmission lines and neural intelligence for effective fault location determination and incipient fault prediction in transmission lines. Simulations considering the NeuroAMI predictor for the PSD signals showed that apart from peaks of about 25V/k-Hz, 27V/k-Hz and 35V/k-Hz, the proposed neural predictor fault location estimates closely matched the expected fault locations. Considering the data-driven approach based on a public dataset, the proposed NeuroAMi technique showed superior RMSE values over the conventional BP-FFANN.

KEYWORDS: Fault localization, Fault detection, Neural intelligence, Power system, Transmission Line

Cite This Paper: Wokoma, B. A., Idoniboyeobu, D. C., Ahiakwo, C. O. & Braide, S. L. (2022). Incipient Fault Localization and Classification for Transmission Lines using Neural Intelligent Technique. *Journal of Newviews in Engineering and Technology*. 4(3), 69 – 76.

1. INTRODUCTION
Power system have for long been berserk with the burden of maintaining a continuous state of uninterrupted energy supply. However, due to various degrees of faults, the tendency to maintain the much-needed power stability status quo has been unachievable. Thus, ongoing researches focus on overcoming the various faults possible in power transmission lines considering specifically the insulation degradation the short-circuit line faults and localizations and the power network component faults such as in transformers (Negrão *et al.*, 2013; Stefenon *et al.*, 2020; Tayeb *et al.*, 2011; Roostaee *et al.*, 2017; Jembari *et al.*, 2019; Mustari *et al.*, 2019; Li *et al.*, 2019; Contreras-Valdes *et al.*, 2020).

While these approaches have proven particularly useful, there has still been the problem of faults leading to catastrophic failures in some instances thereby requiring the preventative actions. As a follow up to this challenge, the incipient determination of faults is currently gaining traction. Thus, researchers find out that it is better to identify the fault earlier through real time monitoring systems considering variety of fault signatures (Andresen *et al.*, 2018).
In this paper, a pragmatic transmission line (TL) monitoring and localization solution is proposed that follows from the theory of resonant frequencies in power transmission lines and neural predictive systems as found in mammalian brains. The idea behind this approach is to marry the continual learning capability of human brains with the sound principles of resonant

transmission lines for effective monitoring and incipient localization of faults in power transmission lines and in real time. With the proposed approach, it should be possible to determine the TL faults in advance and hence safeguard the power network from an imminent collapse.

2. MATERIALS AND METHODS

This section describes the proposed transmission line (TL) resonance model as in section 2.1 and the neural prediction technique employed (see section 2.2). The TL resonance model includes the neural prediction logic in a combined incipient fault monitoring and prediction system.

2.1. Resonance Model of Transmission Line

The resonance model of a TL considering Single-Line-to-Ground faults is based on the equivalent pi connected circuit shown in Figure 1.

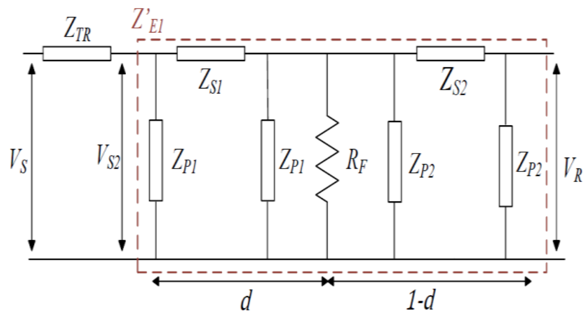

Figure 1. Transmission Line model for resonant studies in presence of SLG faults
(Source: Govindarajan *et al.*, 2015).

In the model of Figure 1, the electrical parameters are distributed along the length of the TL. The core system line parameters of interest for include the line impedances, z, and shunt admittance, γ, which are computed according to (1) and (2):

$$z = R_x + j\omega L_x \quad (1)$$

$$\gamma = j\omega C_x \quad (2)$$

Where:

R_x = Resistance of line per unit length
L_x = Inductance of line per unit length
C_x = Capacitance of line per unit length

If we consider a cable of length say l, the series, and parallel impedances Z_s and Z_p are computed as in (Glover *et al.*, 2012):

$$Z_s = Z_c \sinh(\gamma l) \quad (3)$$

$$Z_p = \frac{\tanh\left(\gamma l/2\right)}{Z_c} \quad (4)$$

where,
γ = line propagation constant
Z_c = line characteristic impedance

Without loading, the time-domain transfer function of the TL system may be represented as:

$$H_c = \frac{V_R}{V_S} = \frac{Z_P}{Z_S + Z_P} = \frac{1}{\cosh(\gamma l)} \quad (5)$$

Using s-function representation, (5) is re-modeled as:

$$H_c(s) = \frac{V_R(s)}{V_S(s)} = \frac{1}{\cosh\left(\sqrt{(R + sL)sC}\right)} \quad (6)$$

Finally, to obtain the resonant frequencies, s_{nc}, the roots of the denominator part in (6) must be solved; the solution is as provided in (7).

$$s_{nc} = -\frac{R}{2L} \pm j\sqrt{\frac{((2n-1)\pi)^2}{4LC} - \frac{R^2}{4L^2}}, \quad n = 1,2,3,\ldots \quad (7)$$

Since at most times, $1/(LC) >> (R/L)^2$, the roots are approximated as in (8):

$$s_{nc} = -\frac{R}{2L} \pm j\frac{(2n-1)\pi}{2\sqrt{LC}}, \quad n = 1,2,3,\ldots \quad (8)$$

Journal of Newviews in Engineering and Technology (JNET)
Volume 4, Issue 3, December 2022
Available online at http://www.rsujnet.org/index.php/publications/2022-edition
e- ISSN: 2795-2215

From (8), a resonant peak will appear when the TL real response frequency is equal to the imaginary part. This follows from theory and the approximate resonant frequencies are (Lin & Holbert, 2009):

$$\omega_{rnc} \cong \frac{(2n-1)\pi}{2\sqrt{LC}}, \qquad n = 1,2,3,\ldots \tag{9}$$

and,

$$f_{rnc} \cong \frac{(2n-1)}{4\sqrt{LC}}, \qquad n = 1,2,3,\ldots \tag{10}$$

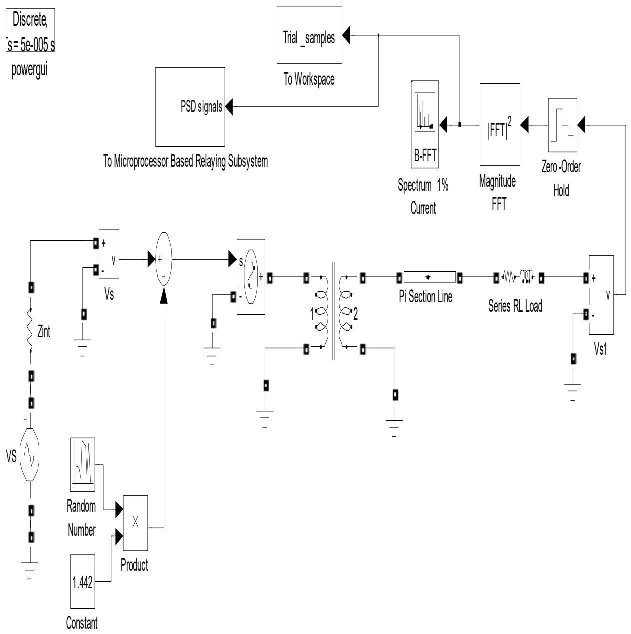

Figure 2. Real Time Simulation model.

2.2. Neural Prediction Technique

The considered neural predictive approach is based on a theory called auditory machine intelligence (AMI) that utilizes the perception of humans to an odd-ball stimulus and intelligent processing in auditory cortex to form invariant predictions in time and space. This approach fundamentally includes the following (Osegi & Anireh, 2019):

i. A set of input detectors.

ii. A processing logic based on Change Detection (CD) and a Model Adjustment (MA) formula.

iii. A learning algorithm using Hebbian style reinforcement rules.

The models in (9) and (10) show that resonant frequencies will occur in odd multiples.

Thus, these models can be used to re-represent further higher dimensions in scale.

A real time systems level simulation model describing the aforementioned operation is as shown in Figure 2.

Using the aforementioned scheme, it is possible to generate continual predictions of a sequence of time-stepped inputs.

The architecture of the proposed AMI neural solution is as shown in Figure 3. In this architecture, mathematical formulas are labeled as an operator sign while functional modules and a trigger block define the key functional routines and time series attributes used in the control initializations of the AMI respectively. A Binary Encoder and Binary-to-Integer Transformer module are used to convert the set of input detectors labeled X_t, from a multivariate to a univariate time series. By default, a Change Detection (CD) mismatch processing function is enabled while the trigger control is set to 0. When a transition is needed from a univariate to a multivariate time series processing, the trigger is enabled and the Model Adjustment (MA) processing of X_t is activated. If the converse is the case, CD processing only is activated.

Journal of Newviews in Engineering and Technology (JNET)
Volume 4, Issue 3, December 2022
Available online at http://www.rsujnet.org/index.php/publications/2022-edition
e- ISSN: 2795-2215

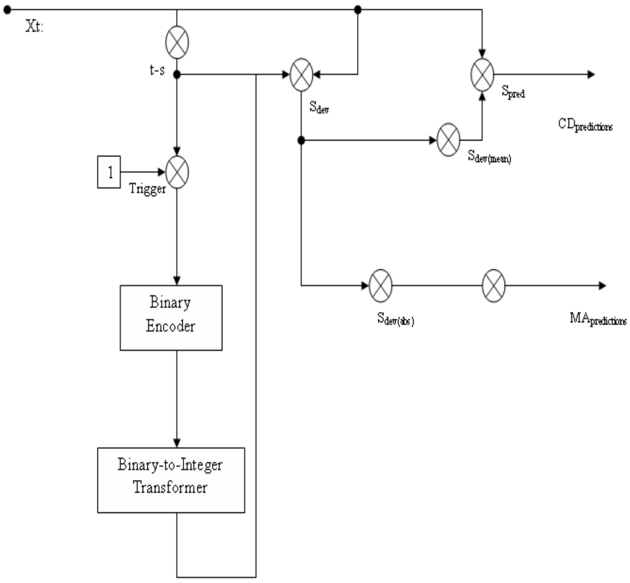

Figure 3. AMI Neural Architecture
(Source: Osegi & Anireh, 2019).

The primary predictions of the Neural AMI solution are described by Phase-1 prediction equations and as follows:

First, we define a mean deviant point as in (11):

$$S_{dev(mean)} = \frac{\left(\left(\frac{\sum [S_{dev}]}{(n-1)} \right) + S_{deviant} \right) - 2}{n+1} \quad (11)$$

where,
n = number of data points in a temporal sequence
$S_{deviant}$ = the *(n-1)th* value of the temporal sequence
S_{dev} = the difference between $S_{deviant}$ and S_{stars}
S_{stars} = the *(n-2)th* values of the temporal sequence
S^* = sparse set of input sequences

Next a prediction is performed using (12):

$$S_{pred} = S_{deviant} + S_{dev(mean)} \quad (12)$$

where,

$$S_{deviant} = S_n^* - 1 \quad (13)$$

$$S_{stars} = S_n^* - 2 \quad (14)$$

The Neural AMI technique processing and learning functions are also as described in Algorithms 1 and 2 respectively.

Algorithm 1. AMI Processing Algorithm
1: Initialize S_{pred}, as prediction parameter, S_{stars}, as input sequences (standards) State, $S_{dev(mean)}$ as deviant mean, j as iteration counter.
2: *for* all s∈ $s.S_{stars}$, & j > 1, do
3: Compute $S_{deviant}$ and S_{stars} using (13) and (14)
4: $S_{dev} \leftarrow \|S_{deviant} - S_{stars}\|$ // deviations from standards
5: Compute $S_{dev(mean)}$ using (11)
6: Compute S_{pred} using (12) and (13)
7: Update $S_{dev(mean)}$ using Algorithm 2
8: *end for*

Algorithm 2. AMI Learning Algorithm
1: Initialize S_{pred}, as prediction parameter, S_{stars}, as input sequences (standards) State, $S_{dev(mean)}$ as deviant mean, $S_{diff(1)}$ as difference between S_{pred}, $S_{Deviant}+1$ and $S_{diff(2)}$ as difference between $S_{dev(mean)}$ and $|S_{diff(1)}|$, l_p as correction factor or bias.
2: *for* all s∈ $s.S_{stars}$ do
3: if $S_{diff(2)} > 0$
4: $S_{dev(mean)} \leftarrow S_{dev(mean)} - |S_{diff(1)}|$ // Weaken deviant mean by a factor, $|S_{diff(1)}|$
5: elseif $S_{diff(2)} < 0$
6: $S_{dev(mean)} \leftarrow S_{dev(mean)} + |S_{diff(1)}|$ // Reinforce deviant mean by a factor, $|S_{diff(1)}|$
7: else
8: $S_{dev(mean)} \leftarrow S_{dev(mean)} + l_p$
9: end if
10: *end for*

2.3. Implementation Details and Datasets

Journal of Newviews in Engineering and Technology (JNET)
Volume 4, Issue 3, December 2022
Available online at http://www.rsujnet.org/index.php/publications/2022-edition
e- ISSN: 2795-2215

The strategy of how to implement the NeuroAMI incipient fault estimation borders on localization using the resonance theory model for a given line and classification considering a publicly available dataset (the VSB power line datasets) which was provided by Ostrava Technical University as a Kaggle competition dataset.
The fault localization data comprised of several sequences of Power Spectral Density (PSD) voltage signals and was synthesized using a real time emulator as shown in Figure 4. To achieve a variety of signals, the simulation was re-run for a number of trial runs and for each trial run, the fault location was varied or kept constant and the corresponding PSD signals recorded. In Table 1, shows the TL parameter specifications used to generate the results.
The VSB datasets consist of Partial Discharge (PD) signal measurements on the three power line phases. A sample of these data set is as shown in Table 2.

Table.1. Key Transmission Line Specifications

Parameter	Value/Specification	Unit
Line Length	138	Km
Circuit type	Single	NA
Conductor cross-section	350	mm^2
Resistance	0.0390	Ω/km
Inductance	1.11	mH/km
Capacitance	912.06	uF/km

Table.2. Sample VSB Kaggle Dataset

Signal_id	id_measurement	Phase	Target
0	0	0	0
1	0	1	0
2	0	2	0
3	1	0	1
4	1	1	1
5	1	2	1
6	2	0	0
7	2	1	0

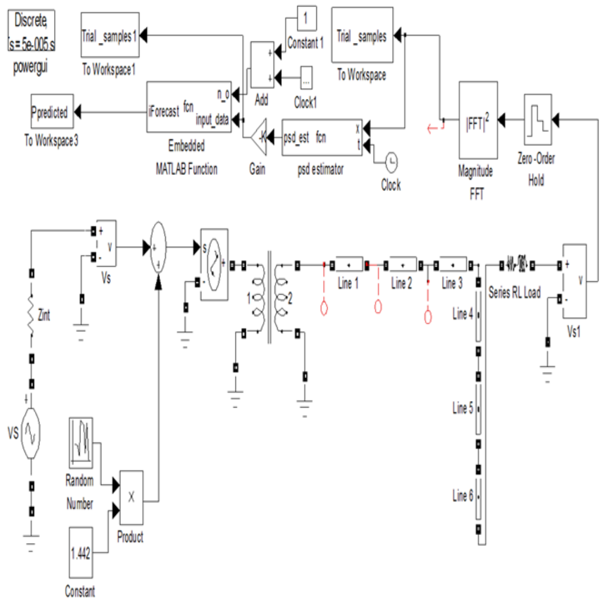

Figure 4. Detailed schematic of the power transmission line for simulation studies.

3. RESULTS AND DISCUSSION

In this section simulations are done in MATLAB/SIMULINK based on existing line parameters of the TL of a section of Nigerian 330kV network (Onitsha-Alaoji single circuit, see Table 1, Section 2, sub-section 2.3) and on the open dataset from the VSB Kaggle repository.

3.1 System Level Simulations - No Fault situation

Considering the detailed schematic in Figure 3, the simulation results is as presented in the graph (Figure 4) showing prediction based on Neuronal Auditory Machine Intelligence (NeuroAMI) technique - an approach of advanced technology in (Osegi & Anireh., 2019; Osegi *et al.*, 2020).

Journal of Newviews in Engineering and Technology (JNET)
Volume 4, Issue 3, December 2022
Available online at http://www.rsujnet.org/index.php/publications/2022-edition
e- ISSN: 2795-2215

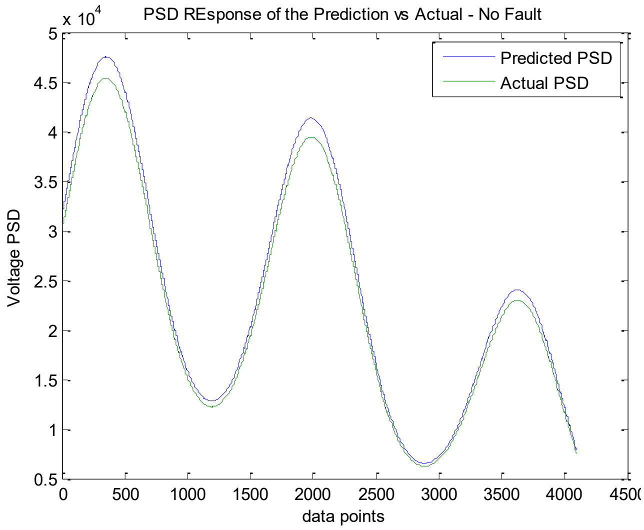

Figure 5. PSD prediction response compared to actual values during no-fault simulation.

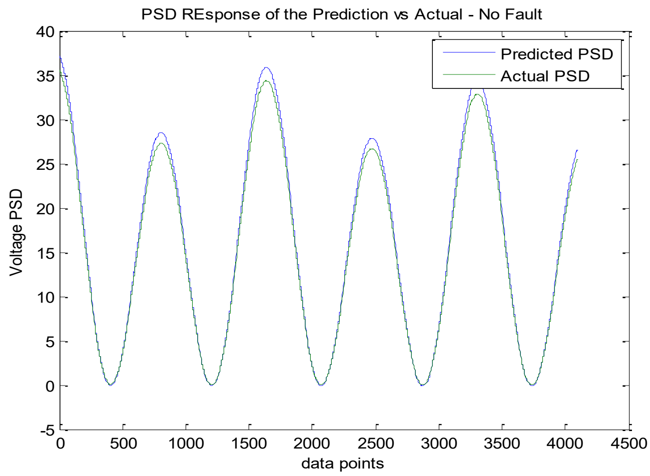

Figure 6. PSD prediction response compared to actual values under fault conditions.

3.2 System Level Simulations – Under Fault situation

In the case of a fault in the transmission line, we consider a fault after line 2 – see the schematic of Figure 4. This corresponds to a fault at a location of 40km from the step-up transformer end and at a resistance of 0.1 Ω. The resulting simulation is as presented in the graph of Figure 5.

The results (response graphs) in Figure 4 and Figure 5 are indicative of the close correlation between the actual PSD estimate and the predicted one. However, at peaks of about 25V/k-Hz, 27V/k-Hz and 35V/k-Hz, there are noticeable discrepancies in the actual vs. predicted estimates during faulted case (see Figure 5).

3.3 Data driven simulations.

Considering incipient fault predictions, data-driven simulations were performed with a small sample data (VSB dataset) in comparison with the standard well known and popular back-propagation trained Feed-Forward Artificial Neural Network (FFANN).

The comparative results were reported in terms of the Root Mean Squared Error (RMSE) as shown in Table 3 for the power lines and for the first 100 samples of VSB dataset. The standard ANN (FFANN) followed the usual convention of training-testing data split with 60% for training and 40% for testing from the considered 100samples and the simulations were performed for 5 trials and the mean computed. Also, a bivariate data splitting method using a scheme earlier proposed in (Osegi, 2021) was employed for the continual learning predictions in the proposed Neuro-AMI technique. In Table 3 is shown the individual trial errors for the different lines as per the FFANN predictions.

From the results of Table 4, the comparative results considering a real world case study data showed the superiority of using proposed technique over the conventional FFANN.

Journal of Newviews in Engineering and Technology (JNET)
Volume 4, Issue 3, December 2022
Available online at http://www.rsujnet.org/index.php/publications/2022-edition
e- ISSN: 2795-2215

Table 3. Comparative RMSE Results using VSB Dataset

Line	AMI_{RMSE}	$FFANN_{RMSE}$
1	0.3742	0.5428
2	0.3742	0.4628
3	0.3464	0.6628

Table 4. FFANN RMSE for different trial runs and lines using VSB dataset

Trials	FFANN RMSE(1)	FFANN RMSE(2)	FFANN RMSE(3)
1	0.6363	0.3747	0.5027
2	0.4800	0.7221	0.6983
3	0.4730	0.5404	0.8559
4	0.3675	0.3745	0.4053
5	0.3571	0.7025	0.8518

4. CONCLUSION

This research paper has proposed a Neural auditory machine intelligence (AMI) approach and simulation model to TL fault diagnosis in power system transmission network. It has also presented some initial results on the developed solution model and the results showed good predictive response of the considered approach.
Currently, this research work is ongoing at the Department of Electrical Engineering, Rivers State University, Nigeria. Future work will incorporate real-time embedded microprocessor relaying logic to further enhance the proposed model features. Also, the proposed approach should be applied to different line configurations considering the varieties of existing line length and considering the gradual variation of the fault resistances.

5. ACKNOWLEDGEMENTS

Sincere thanks and acknowledgment go to Engr. Osegi, E. N. who assisted with code modifications for the simulations.

REFERENCES

Andresen, C. A., Torsaeter, B. N., Haugdal, H., & Uhlen, K. (2018). Fault detection and prediction in smart grids. In *2018 IEEE 9th International Workshop on Applied Measurements for Power Systems (AMPS)* (pp. 1-6). IEEE.

Contreras-Valdes, A., Amezquita-Sanchez, J. P., Granados-Lieberman, D., & Valtierra-Rodriguez, M. (2020). Predictive data mining techniques for fault diagnosis of electric equipment: a review. *Applied Sciences*, *10*(3), 950.

Glover, J. D., Sarma, M., & Overbye, T. J. (2012). Transmission Lines: Steady-State Operation. *Power System Analysis and Design*, 254-262.

Govindarajan, S., Kim, Y., & Holbert, K. E. (2015). A novel methodology for power cable monitoring using frequency domain analysis. In *2015 North American Power Symposium (NAPS)* (pp. 1-6). IEEE.

Jembari, N. N., Yi, S. S., Utomo, W. M., Zin, N. M., Zambri, N. A., Mustafa, F., ... & Buswig, Y. M. (2019). IoT Based Three Phase Fault Analysis for Temporary and Permanent Fault Detection. *Journal of Electrical Power and Electronic Systems*, *1*(2).

Lin, K., & Holbert, K. E. (2009). Applying the equivalent pi circuit to the modeling of hydraulic pressurized lines. *Mathematics and Computers in simulation*, *79*(7), 2064-2075.

Li, M., Yu, Y., Ji, T., & Wu, Q. (2019). On-line Transmission Line Fault Classification using Long Short-Term Memory. In *2019 IEEE 12th International Symposium on Diagnostics for Electrical Machines, Power Electronics and Drives (SDEMPED)* (pp. 513-518). IEEE.

Mustari, M. R., Hashim, M. N., Osman, M. K., Ahmad, A. R., Ahmad, F., & Ibrahim, M. N. (2019). Fault Location Estimation on Transmission Lines using Neuro-Fuzzy System. *Procedia Computer Science*, *163*, 591-602.

Negrao, M. M. L., da Silva, P. R. N., Gomes, C. R., Gomes, H. S., Junior, P. V., & Sanz-Bobi, M. A. (2013). MCHO–A new indicator for insulation conditions in transmission lines. *International Journal of Electrical Power & Energy Systems*, *53*, 733-741.

Osegi, 2021 Using Hierarchical

Osegi, E. N., & Anireh, V. I. (2019). AMI: An Auditory Machine Intelligence Algorithm for Predicting Sensory-Like Data. *Computer Science*, *5*(2), 71-89.

Osegi E. N., Taylor O. E., Wokoma B. A., Idachaba, A. O. (2020). A Smart Grid Technique for Dynamic Load Prediction in Nigerian Power Distribution Network. In: Pandit M., Srivastava L., Venkata Rao R., Bansal J. (eds) Intelligent Computing Applications for Sustainable Real-World Systems. *ICSISCET 2019. Proceedings in Adaptation, Learning and Optimization*, vol 13. Springer, Cham. https://doi.org/10.1007/978-3-030-44758-8_38

Roostaee, S., Thomas, M. S., & Mehfuz, S. (2017). Experimental studies on impedance-based fault location for long transmission lines. *Protection and Control of Modern Power Systems*, *2*(1), 1-9.

Stefenon, S. F., Ribeiro, M. H. D. M., Nied, A., Mariani, V. C., dos Santos Coelho, L., da Rocha, D. F. M., Grebogi, R. B. & de Barros Ruano, A. E. (2020). Wavelet group method of data handling for fault prediction in electrical power insulators. *International Journal of Electrical Power & Energy Systems*, *123*, 106269.

Tayeb, E. B. M., & Rhim, O. A. A. A. (2011). Transmission line faults detection, classification and location using artificial neural network. In *2011 International Conference & Utility Exhibition on Power and Energy Systems: Issues and Prospects for Asia (ICUE)* (pp. 1-5). IEEE.